

Ab initio study of hydrogen interaction with pure and nitrogen-doped carbon nanotubes

Zhiyong Zhang and Kyeongjae Cho*

Department of Mechanical Engineering, Stanford University, Stanford, California 94305, USA

(Received 31 October 2006; revised manuscript received 3 December 2006; published 21 February 2007)

Detailed studies of mechanisms for hydrogen dissociative adsorption and diffusion on pure and nitrogen-doped (8, 0) carbon nanotubes are carried out using the first-principles density functional theory method. (1) For pure carbon nanotubes, we have identified the energetically most favorable dissociative pathway for hydrogen adsorption, with a barrier height of 1.3 eV. We also found that the adsorbed hydrogen atoms can act as an autocatalyst for further dissociative adsorption of hydrogen molecules. (2) It is found that on pure carbon nanotubes the diffusion of hydrogen atoms is constrained by interaction with neighboring adsorbed hydrogen atoms. The diffusion barrier is around 0.7 eV for an isolated hydrogen atom, but becomes substantially higher at around 1.4 eV in the presence of adsorbed hydrogen in neighboring positions. (3) Doping the nanotube with nitrogen considerably alters the catalytic effects of the carbon nanotube for hydrogen dissociative adsorption. The dissociative adsorption of hydrogen on the carbon nanotube is greatly enhanced, with the barrier substantially reduced to ca. 0.9 eV. The differences in the barrier heights are explained through analysis of the electronic structure changes of the nanotube.

DOI: 10.1103/PhysRevB.75.075420

PACS number(s): 61.46.Fg

I. INTRODUCTION

Since first reported in 1991,^{1,2} carbon nanotubes (CNTs) have spurred tremendous activities in both fundamental and applied-technology studies and opened up seemingly endless possibilities of physical, chemical, biological, and medicinal applications. As results of the characteristically strong covalent bonding and topologically unique one-dimensional structure with variable nanometer-sized diameter and chirality, CNTs exhibit extraordinary physical and chemical properties. Initial studies of CNTs revealed their superior mechanical strength,^{3–5} thermal conductivity,⁶ and outstanding field emission properties.^{7,8} Depending on the chirality, CNTs can either be metallic and transport currents without thermal dissipation or be semiconducting.⁹ The chemical properties and chemical functionalization of CNTs, important for preparation, purification, and separation according to their size and chirality, as well as various biological and chemical applications, have also received increasing attention.^{10,11} In particular, the chemical reactivity of CNTs has been a subject of intense studies for the potential use of CNTs as hydrogen storage material^{12,13} and catalytic^{14,15} and support material¹⁶ for fuel cell electrodes in energy-related applications.

Since the first demonstration of hydrogen storage in CNTs, there have been continued efforts to understand the hydrogen storage capability of CNTs, with both physisorption and chemisorption as possible mechanisms. The maximal chemisorption capability, with a one-to-one ratio of hydrogen to carbon, gives rise to a storage capability of ca. 7.7 wt %. However, the dissociative adsorption of hydrogen is associated with a substantial energy barrier.^{17–19} To have a realistic hydrogen storage material, it is important to reduce the energy barrier for hydrogen dissociation so that the adsorption and desorption of hydrogen are easily reversible at ambient temperature and pressure. Transition metal nanoparticles can be used as catalysts to facilitate reversible chemisorption of hydrogen on CNTs. Transition metal catalysts, dispersed on the CNTs, can act as catalyst to break up the

hydrogen molecule easily, and the hydrogen atoms can then diffuse along the CNT and saturate the entire CNT through the so-called spill-over mechanism. Up to now, however, the mechanisms for hydrogen dissociation and diffusion on CNTs are not well-understood, and systematic studies are still lacking.

With their superior mechanical strength, thermal and electrical conductivity, and high surface area and porosity, CNTs have also attracted increasing interests for their catalytic properties, primarily for potential applications as catalysts and/or catalyst supports for fuel cell electrodes.^{14,15,20} The catalytic properties of CNTs have been explored for various other applications also, including methane decomposition, oxidative dehydrogenation of ethylbenzene to styrene, oxidation of *p*-toluidine, and conversion of aniline to azobenzene.^{21–26} The reactivity of the CNTs is mostly determined by two effects: curvature-induced pyramidalization and misalignment of the π orbital.^{27,28} CNTs are relatively inert, with reactivity lying between planar graphite and spherical fullerenes. There have been continued efforts to modify the reactivity of CNTs so that CNTs can be processed and modified to have the desired properties. There are increasing evidences showing that the electrical properties are extremely sensitive to charge transfer and chemical doping effects by various molecules. Substitutional doping, with dopants incorporated directly in the CNTs, is the most desirable way to modify the chemical activities of CNTs since it maintains the robust framework of the CNT and most of its intrinsic properties.^{11,29} The objective of this study is to elucidate the intrinsic chemical reactivity of CNTs, particularly for hydrogen dissociation on pure and nitrogen doped CNTs, and the property of hydrogen diffusion on the CNTs.

II. COMPUTATIONAL DETAILS

The DFT results are calculated using the VASP code,³⁰ with the local density approximation of Ceperley and Alder³¹ as parametrized by Perdew and Zunger.³² Blochl's projector augmented wave (PAW) potentials³³ are used to describe the

TABLE I. Comparison of barrier heights with low and high plane wave cutoff. C2C3: dissociative adsorption on C2 and C3. C1C4: dissociative adsorption on C1 and C4. C1C4/C2C3: dissociative adsorption on C1C4 when C2 and C3 are hydrogenized. Single N: dissociative adsorption over C1 and C4 when N is doped at C2 position.

	C2C3	C1C4	C1C4/C2C3	Single N
Low cutoff	2.73	1.33	0.89	0.91
High cutoff	2.82	1.44	0.89	1.00

ion-electron interactions. The PAW potentials are taken from the database provided through the VASP package, and an energy cutoff of 286.57 eV is used throughout. A test with a higher cutoff at 500 eV shows that the largest change in barrier height is around 0.11 eV and the effects on barrier height by doping and hydrogenation remain essentially the same (see Table I for details). All the calculations are done for the zigzag (8, 0) tube and two primitive unit cells are used to reduce the finite-size error and to minimize the interaction among the adsorbates. At least five k -points in the direction of the tube axis are used in the simulations, with a supercell size of $14.264 \times 14.264 \times 14.264 \text{ \AA}^3$. Geometry optimizations are converged to forces on atoms less than 0.001 eV/\AA , and electronic energies are converged to 0.0005 eV. To obtain the reaction profile, the climbing image nudged elastic band (NEB) method is applied to locate the reaction pathways and transition states.³⁴

III. RESULTS AND DISCUSSION

A. Optimal hydrogen dissociation pathway

To obtain the optimal reaction path for the dissociation of hydrogen on a CNT, several hydrogen adsorption configurations are explored. From our calculations, we found that the energetically most favorable hydrogen adsorption sites for a pair of hydrogen are the C2 and C3 positions of the six-member ring, as shown in Fig. 1. Three low energy configurations are indicated in Fig. 1. The calculated binding energies, defined relative to an isolated H_2 molecule and CNT, range from -0.045 to 0.276 eV, with positive binding energies indicating an energetically stable configuration. We ex-

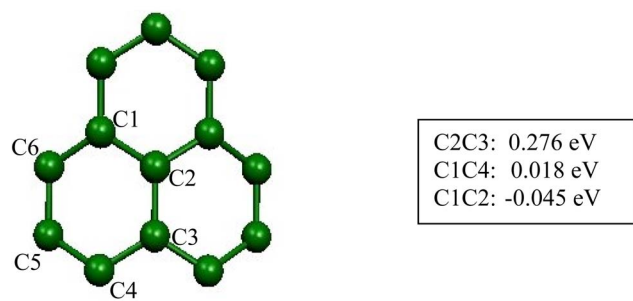


FIG. 1. (Color online) Low-energy configurations of pairs of hydrogen on a CNT. The first two configurations are bound against an isolated CNT and hydrogen molecule.

amined the hydrogen dissociative adsorption reaction profiles of all three configurations. The initial configurations of H_2 are chosen to be 3.5 \AA away from the CNT, with the H_2 direction oriented parallel to the two C atoms in the adsorbed configurations. The calculated reaction profiles are shown in Fig. 2. The calculated reaction energy barriers are 1.33, 2.38, and 2.73 eV for the three adsorbed configurations C1C4, C1C2, and C2C3, respectively. The most stable configuration, C2C3 is associated with the highest energy barrier, and the lowest energy barrier is found for the least stable configuration C1C4. In a previous study, H dissociative adsorption on a (5, 5) CNT was considered, and they obtained energy barriers of ca. 3.07 eV for the C2C3 pathway and 2.7 eV for the C2C5 pathway.¹⁹ However, they did not consider the pathway corresponding to dissociation on C1C4.

The reactivity of the CNT is mostly determined by the strain due to the curvature of the tube and the π orbital misalignment.²⁸ The C atom in the CNT is in a configuration that lies in between sp^2 and sp^3 hybridization. Chemisorption on a C atom will release the strain and changes the C atomic bonding structure to very close to sp^3 . Chemisorption also changes the configuration of the surrounding C atoms considerably, releasing much of the constraint inherent in a perfect CNT. As a result, the chemical reactivity of the surrounding C atoms is expected to be considerably changed. This effect is reflected in the much stronger binding energy for a pair of hydrogen atoms chemisorbed in the neighboring positions of a pair of chemisorbed H atoms. We also examined the effect of the chemisorption on further dissociative adsorption. While a pair of hydrogen atoms is adsorbed at the most stable configuration, C2C3 as shown in Fig. 1, we computed the reaction profile for the dissociation of the second pair of hydrogen atoms on the C1 and C4 positions. The reaction profile is shown in Fig. 3. It is seen that the energy barrier for the adsorption of a second pair of hydrogen atoms, in the presence of a first pair of hydrogen atoms adsorbed in a neighboring position, is considerably lowered to 0.89 eV from 1.33 eV.

B. Hydrogen diffusion on CNT

Another important issue to understand is how hydrogen will diffuse once it is chemisorbed on the CNT. Chemisorbed hydrogen atoms tend to stay in clusters, as our calculations show (e.g., two H atoms on C2C3 sites are more stable than C1C4 sites by 0.25 eV). Isolated chemisorbed hydrogen may diffuse on the CNT to form larger clusters and/or stripes of lower energy configurations. It is likely that, in the case of using CNT as hydrogen storage material, catalysts will be required to break the hydrogen molecule and facilitate the hydrogenation process. The most likely mechanism is the diffusion of hydrogen from the hydrogen adsorption sites to cover the remote part of the CNT. Chemisorbed hydrogen forms a strong covalent bond with the C atom of a CNT, but hopping of hydrogen from one site to a neighboring site might still be relatively easy since no C–H bonds are completely broken during this process. For the diffusion of single isolated hydrogen this is indeed the case as shown in our calculation, and the calculated barrier for a single isolated

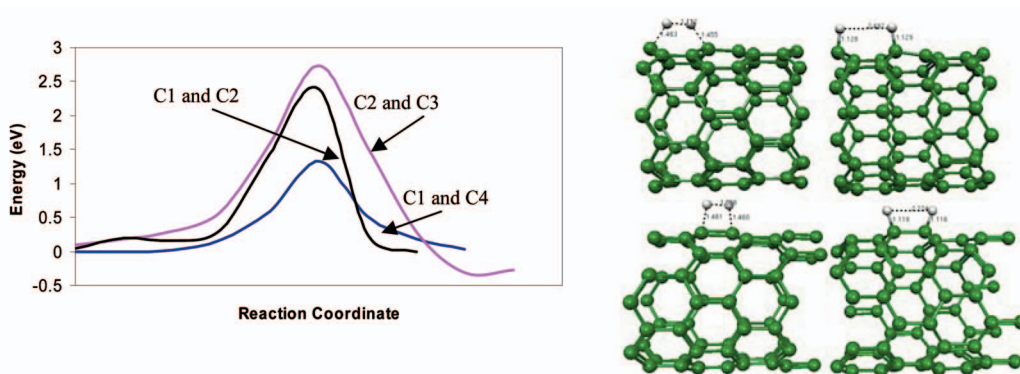


FIG. 2. (Color) Reaction profiles for H₂ dissociation on a CNT for the three configurations shown in Fig. 1. Red: C2C3, black: C1C2, and blue: C1C4. The barrier heights for the three configurations C2C3, C1C2, and C1C4 are 2.73, 2.38, and 1.33 eV, respectively. The reaction coordinates are the images between the initial and final states. The right panel shows the structures of the transition states (left) and the final adsorbed states (right): upper right: dissociation over C1 and C4 and lower right: dissociation over C2 and C3.

hydrogen atom to hop to neighboring sites is relatively low at 0.70 eV.

On the other hand, the diffusion of hydrogen in a stable pair configuration is a much more difficult process. Starting from various initial pair configurations, we have explored the possible pathways of hydrogen diffusion to form a new pair of configurations, and some of the results are shown in Fig. 4 together with the reaction profile for single isolated hydrogen diffusion. In particular we examined the diffusion profile from the C1C4 configuration to the C2C3 configuration, as the former is the configuration with the lowest barrier to hydrogen dissociative chemisorption and the later corresponds to the most stable configurations for a pair of chemisorbed hydrogen atoms. The concerted pathway, with the two hydrogen atoms moving in concert, is associated with a high energy barrier of 3.20 eV and thus can be ruled out. In the two-step pathway, H at C1 to C2 position followed by H at C4 to C3 position, the first step has a barrier of ca. 1.4 eV and there is an intermediate configuration that is about 0.78 eV above the initial configuration. The second step, from the metastable intermediate to the final configuration, is associated with a rather low barrier of only 0.4 eV. Thus the most likely pathway from the configuration of easy hydrogen dissociation to the stable configuration is through a two-step process, with the first step being the rate limiting step.

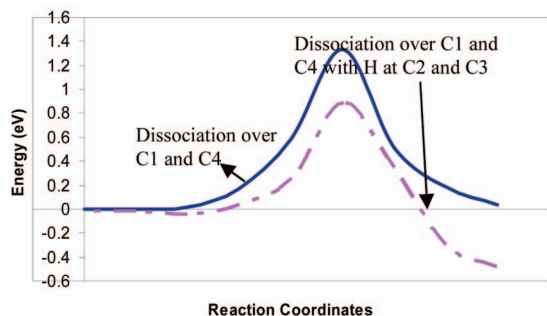


FIG. 3. (Color) Solid line: pure CNT, H dissociation over C1 and C4, energy barrier 1.33 eV. Dashed line: H dissociation on C1 and C4 with hydrogen atoms chemisorbed on C2 and C3 positions, energy barrier: 0.89 eV.

C. Reactivity of doped CNT

As discussed in the previous paragraphs, chemisorption of hydrogen can change the reactivity of the neighboring sites on a CNT and makes the dissociation of hydrogen on these sites much easier. Still, there is a high energy barrier associated with the initial dissociative adsorption. One way to modify the chemical reactivity is by doping the CNT. We have considered various configurations of doping the CNT with N atoms, including doping with a single N atom and with two N atoms at C2C3, C3C6, and C2C6 positions (refer to Fig. 1 for the numbering of atomic positions). The results for the energy barriers and adsorption energies are summarized in Table II. Our results show that when doped with N, the reactivity of the CNT changes substantially and the changes depend strongly on the configurations of the dopants. In all the calculation for doping, we used a simulation cell that consists of two primitive cells. The dissociation pathway investigated is along the C1 and C4 position, the pathway that gives the lowest barrier to dissociation, as discussed in previous paragraphs. The reaction profiles for a singly doped CNT are shown in Fig. 5.

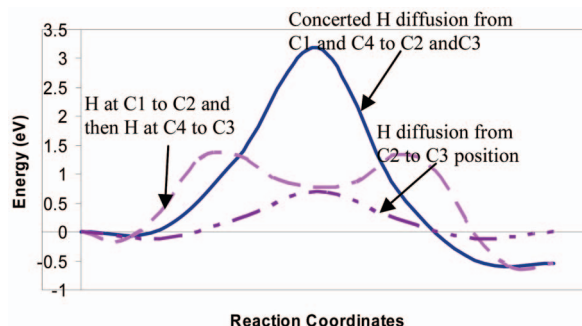


FIG. 4. (Color) Hydrogen diffusion pathways on CNT. Brown: single isolated H on the C2 position diffuses to the C3 position, barrier height around 0.70 eV. Blue: C1C4 to C2C3: concerted diffusion of two hydrogen atoms at C1 and C4 to C2 and C3 positions, barrier height 3.20 eV. Brown: two step diffusion with H at C1 to C2 position and then H at C4 to C3 position barrier heights around 1.4 eV. The intermediate state is ca. 0.7 eV above the initial state.

TABLE II. Binding energy and reaction barriers for hydrogen dissociation to C1 and C4 sites on pure and doped CNT. Energies are in eV.

	Pure CNT	Single N at C2	N at C2 and C3	N at C3 and C6	N at C2 and C6
Barrier height	1.33	0.91	1.29	1.23	0.96
Adsorption energy	0.018	0.05	0.46	0.10	0.19

In the case of doping with a single N at C2 position, it is found that the energy barrier to hydrogen dissociative adsorption to C1 and C4 is substantially reduced, from 1.33 eV for a pure CNT to 0.9 eV for a doped CNT. The binding energy relative to an isolated CNT (doped) and hydrogen molecule is little changed at 0.05 eV, compared with that for a pure CNT at 0.018 eV (a positive number indicates an energetically stable configuration). We also considered various configurations with two neighboring N impurities on the CNT, with two N atoms at the C2C3, C2C6, and C3C6 positions. The CNT with C3C6 N atom substitution is the most stable and the C2C6 substitution is 0.02 eV higher in energy. The configuration with C2C3 N atom substitution is the least stable and much higher in energy by 0.88 eV. When the two N atoms are doped at C2 and C6 positions, there is a substantial change in the reaction barrier for hydrogen dissociation to C1 and C4 sites, compared with that of a pure CNT. The barrier height of ca. 0.96 eV is similar to that of 0.91 eV for a N atom doped in the CNT. The calculated binding energy is ca. 0.19 eV, larger than that of either the case of a pure CNT or the case with a single N dopant. When the two N atoms are doped at either the C3C6 or C2C3 positions, the barrier heights are at 1.23 and 1.29 eV, respectively, little changed compared with the barrier height of 1.33 eV for a pure CNT. On the other hand, the binding energy in the case of C2C3 substitution, where the two N atoms form a N–N bond in the CNT network, is much higher at 0.46 eV. The binding energy for a hydrogen pair in the case of C3C6 substitution is at 0.1 eV, only slightly increased from the pure CNT case. In summary, some special configurations of pair substitution of N in a single hexagon of the CNT can cause substantial changes in binding energy and/or barrier height for hydrogen dissociation.

D. Electronic origin of the differences in hydrogen dissociation reaction

The origin of the differences in the barriers of hydrogen dissociative adsorption on carbon nanotubes can be under-

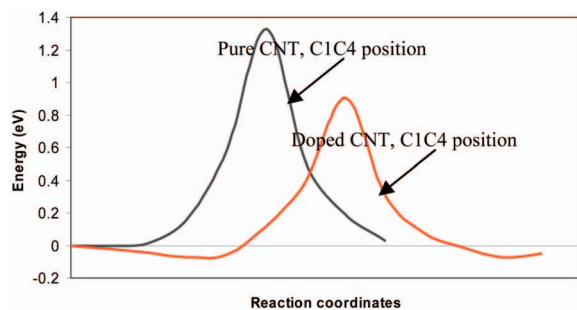


FIG. 5. (Color) Hydrogen dissociation on N doped CNT. Black: pure CNT, energy barrier 1.33 eV over C1 and C4. Red: singly doped N at the C2 position in Fig. 1, Energy barrier: 0.91 eV.

stood by examining the electronic structures through the analysis of local density of states (LDOS). Figure 6 shows the local density of states of the hydrogen and the carbon

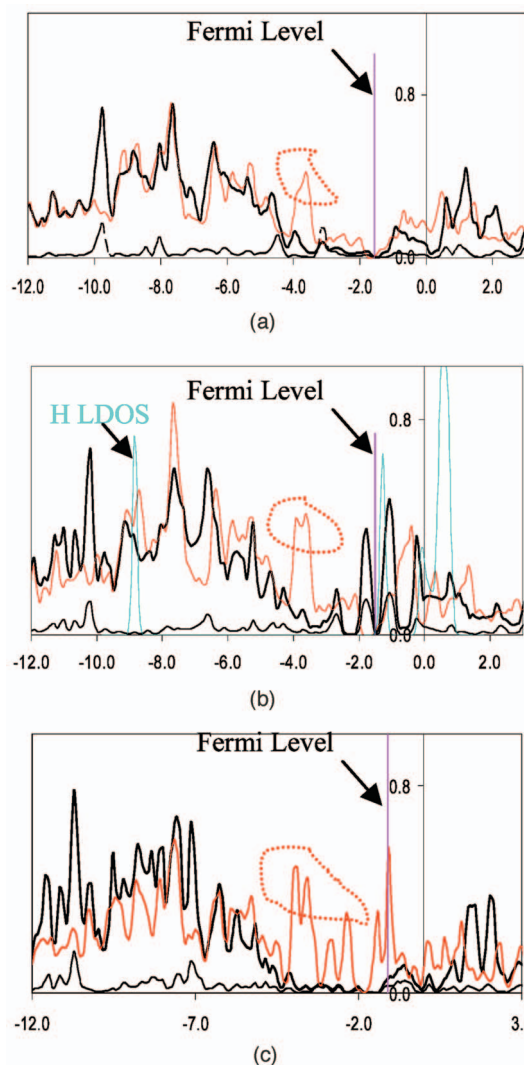


FIG. 6. (Color) Local density states of the carbon and hydrogen atoms involved in bonding at the transition states. (a) H₂ dissociation over C1 and C4. (b) H₂ dissociation over C2 and C3. (c) H₂ dissociation over C1 and C4, N doped CNT. The dotted circles indicate the C states (the C p_⊥ band) that participate strongly in bonding with H in the transition states. The vertical lines indicate the Fermi level. In (b), the local density of states of the isolated H₂, at the same positions as in the transition state configuration, is also shown. The black curves are the LDOS for carbon and hydrogen at the transition states. The red curves are for the same C atoms in the CNT without H, with CNT fixed at the same positions as in the transition states.

atoms upon which the hydrogen molecule dissociates and adsorbs for dissociation through the C1C4 pathway [case 1, Fig. 6(a)] and the C2C3 pathway of the pure CNT [case 2, Fig. 6(b)] and the C1C4 pathway of the nitrogen doped CNT [case 3, Fig. 6(c)]. The interaction between the hydrogen and CNT atom is mainly determined by the bonding and antibonding interactions between the σ_g and σ_u states of hydrogen and p states perpendicular to the CNT (p_\perp), close to the Fermi level, of carbon atoms at bonding position with the hydrogen atoms. The LDOS of the C between the Fermi level and ca. 2 eV below can be easily identified as the C states that participate strongly in bonding with hydrogen as they disappear in the plots of LDOS for interacting CNT and hydrogen, and we refer to these as the C p_\perp band. The strength of the interaction and thus the trends in the barrier heights can be rationalized by considering the positions and weights of the bonding and antibonding states between the carbon p_\perp bands and the hydrogen states. At positions of the bands due to the interaction between C and H, there are obvious differences in the LDOS of the C atoms with and without hydrogen. At other positions, the LDOS of C remain almost identical with and without H. Based on the positions of the C–H bands, relative to the position of the states in an isolated H as shown in Fig. 6(b) for case 2, the characters of these bands can be easily assigned. The lowest C–H bands around -10 eV are obviously due to the interaction of the H σ_g state and the C p_\perp state. The second lowest C–H band, between -8 and -6 eV, is mostly due to the bonding interaction between the H σ_u and the C p_\perp states since they are above the H σ_g state. The highest C–H bands are the results of a combination of the interactions mainly between the C p_\perp and H σ_u and between the H σ_u and the antibonding C p_\perp above the Fermi level. It is mainly the positions and weights of the highest C–H band that largely determine the strength of the interaction and the bonding/antibonding character and thus determine the barrier heights of the transition states. Specifically, in case 2, there is a large occupied C–H band right below the Fermi level and the lowest two C–H bands are considerably smaller than in the other two cases, consistent with the highest barrier height calculated for this case. Case 1 corresponds to the lowest barrier heights for dissociation on the pure CNT and it is observed that the third C–H band lies considerably below the Fermi level at -3 and -4 eV with mostly bonding character. Besides, the two lowest C–H bands are considerably larger in weight. When N is doped in the CNT, three distinctive features contribute to the

further lowering of the barrier height: (1) the C p_\perp band that participates in bonding with H is considerably more extensive, spanning the range from -4 eV right to the Fermi level, due to the extra electron of the N; (2) the interaction between C and H is much stronger, as can be seen by the extensive region of the C LDOS that shows considerable difference with and without hydrogen; and (3) the higher lying C–H band below the Fermi level is completely missing in this case. Finally we note that the calculated barrier heights decrease with the distances between the center of the C p_\perp band and the Fermi level, with the distances between the C p_\perp and the Fermi level at 2.22 eV for case 2, 1.97 eV for case 1, and up to the Fermi level for case 3. Similar correlations with the metal d band positions are extensively used to explain the reactivity of transition metal surfaces.³⁵

IV. CONCLUSION

In summary, we have studied the reactivity of a pure and doped (8, 0) CNT, including binding energies, reaction barriers for hydrogen dissociation, and hydrogen diffusion on the CNT. We have found that for the hydrogen dissociation, the optimal pathway is dissociation and chemisorption on the C1 and C4 positions of the hexagon in the CNT. Chemisorption of hydrogen also modifies the local reactivity of neighboring atoms in the CNT, as exemplified by the increase of binding energy and substantial decrease of energy barrier for further H_2 dissociation and adsorption when a first pair of hydrogen atoms is chemisorbed on the CNT. We also studied the detailed diffusion mechanism of hydrogen on a CNT. We found that a single isolated H is relatively easy to diffuse on the CNT but it is difficult for H in a stable adsorbed cluster to diffuse, even if the diffusion is to an energetically more stable position. Our results show that doping the CNT with nitrogen significantly changes the reactivity of the CNT and reduces the energy barrier for hydrogen dissociation.

ACKNOWLEDGMENTS

We acknowledge Global Climate and Energy Projects (GCEP), at Stanford University for financial support. This research was performed in part using the Molecular Science Computing Facility (MSCF) in Environmental Molecular Sciences Laboratory (EMSL), a national scientific user facility sponsored by the U.S. Department of Energy (DOE), Office of Biological and Environmental Research (OBER) and located at Pacific Northwest National Laboratory (PNNL).

*Present address: Departments of Physics and Electrical Engineering, University of Texas at Dallas, Richardson, TX 75083, USA. Email address: kjeho@utdallas.edu

¹S. Iijima and T. Ichihashi, *Nature (London)* **363**, 607 (1993).

²D. S. Bethune, C. H. Kiang, M. S. de Vries, G. Gorman, R. Savoy, J. Vazquez, and R. Bevers, *Nature (London)* **363**, 605 (1993).

³M. F. Yu, B. S. Files, S. Arepalli, and R. S. Ruoff, *Phys. Rev. Lett.*

84, 5552 (2000).

⁴C. Wei, K. Cho, and D. Srivastava, *Appl. Phys. Lett.* **82**, 2512 (2003).

⁵C. Wei, K. Cho, and D. Srivastava, *Phys. Rev. B* **67**, 115407 (2003).

⁶J. Hone, B. Batlogg, Z. Benes, A. T. Johnson, and J. E. Fischer, *Science* **289**, 1730 (2000).

⁷W. A. de Heer, A. Chatelain, and D. Ugaarte, *Science* **270**, 1179

- (1995).
- ⁸A. Nojeh, B. Shan, K. Cho, and R. F. W. Pease, *Phys. Rev. Lett.* **96**, 056802 (2006).
- ⁹J. Hu, T. W. Odom, and C. M. Lieber, *Acc. Chem. Res.* **32**, 435 (1999).
- ¹⁰S. Peng, K. Cho, P. Qi, and H. Dai, *Chem. Phys. Lett.* **387**, 271 (2004).
- ¹¹S. Peng and K. Cho, *Nano Lett.* **3**, 513 (2003).
- ¹²A. C. Dillon, K. M. Jones, T. A. Bekkedahl, C. H. Kiang, D. S. Bethune, and M. J. Heben, *Nature (London)* **386**, 377 (1997).
- ¹³C. Liu, Y. Y. Fan, M. Liu, H. T. Cong, H. M. Cheng, and M. S. Dresselhaus, *Science* **286**, 1127 (1999).
- ¹⁴M. F. R. Pereira, J. L. Figueiredo, J. J. M. Orfao, P. Serp, P. Kalck, and Y. Kihn, *Carbon* **42**, 2807 (2004).
- ¹⁵S. Maldonado and K. J. Stevenson, *J. Phys. Chem. B* **109**, 4707 (2005).
- ¹⁶C. Wang, M. Waje, X. Wang, J. M. Tang, R. C. Haddon, and Y. Yan, *Nano Lett.* **4**, 345 (2004).
- ¹⁷K. Tada, S. Furuya, and K. Watanabe, *Phys. Rev. B* **63**, 155405 (2001).
- ¹⁸S. Chan, G. Chen, X. G. Gong, and Z. Liu, *Phys. Rev. Lett.* **87**, 205502 (2001).
- ¹⁹E. Lee, Y. Kim, Y. Jin, and K. Chang, *Phys. Rev. B* **66**, 073415 (2002).
- ²⁰P. Serp, M. Corrias, and P. Kalck, *Appl. Catal., A* **253**, 337 (2003).
- ²¹N. Muradov, *Catal. Commun.* **2**, 89 (2001).
- ²²N. Maksimova, G. Mestl, and R. Schlogl, *Stud. Surf. Sci. Catal.* **133**, 383 (2001).
- ²³G. Mestl, N. I. Maksimova, N. Keller, V. V. Roddatis, and R. Schlogl, *Angew. Chem., Int. Ed.* **40**, 2066 (2001).
- ²⁴N. Keller, N. I. Maksimova, V. V. Roddatis, M. Schur, M. G. Mestl, Y. V. Butenko, V. L. Kuznetsov, R. Schlögl, *Angew. Chem., Int. Ed.* **41**, 1885 (2002).
- ²⁵M. Croston, J. Langston, R. Sangoi, and K. S. V. Santhanam, *Int. J. Nanosci.* **1**, 277 (2002).
- ²⁶M. Croston, J. Langston, G. Takacs, T. C. Morrill, M. Miri, K. S. V. Santhanam *et al.*, *Int. J. Nanosci.* **1**, 285 (2002).
- ²⁷S. Niyogi, M. A. Hamon, H. Hu, B. Zhao, P. Bhowmik, R. Sen, M. E. Itkis, and R. C. Haddon, *Acc. Chem. Res.* **35**, 1105 (2002).
- ²⁸S. Park, D. Srivastava, and K. Cho, *Nano Lett.* **3**, 1273 (2003).
- ²⁹M. Terronesa, A. Joriob, M. Endoc, A. M. Raod, Y. A. Kimc, T. Hayashic, H. Terronesa, J.-C. Charliere, G. Dresselhausf, and M. S. Dresselhausg, *Mater. Today* **7**, 30 (2004).
- ³⁰G. Kresse and J. Hafner, *Phys. Rev. B* **47**, 558 (1993); G. Kresse and J. Furthmuller, *ibid.* **54**, 11169 (1996).
- ³¹D. M. Ceperley and B. J. Alder, *Phys. Rev. Lett.* **45**, 566 (1980).
- ³²J. P. Perdew and A. Zunger, *Phys. Rev. B* **23**, 5048 (1981).
- ³³P. E. Blochl, *Phys. Rev. B* **50**, 17953 (1994).
- ³⁴H. Jonsson, G. Mills, and K. W. Jacobsen, in *Classical and Quantum Dynamics in Condensed Phase Simulations*, edited by B. J. Berne, G. Ciccotti, and D. F. Coker (World Scientific, Singapore, 1998).
- ³⁵B. Hammer and J. K. Norskov, *Surf. Sci.* **343**, 211 (1995).